J Radioanal Nucl Chem (2011) 290:289–295
DOI 10.1007/s10967-011-1315-4

The comparison of four neutron sources for Prompt Gamma Neutron Activation Analysis (PGNAA) in vivo detections of boron

J. G. Fantidis · G. E. Nicolaou · C. Potolias · N. Vordos · D. V. Bandekas

Received: 11 March 2011 / Published online: 17 July 2011

Abstract A Prompt Gamma Ray Neutron Activation Analysis (PGNAA) system, incorporating an isotopic neutron source has been simulated using the MCNPX Monte Carlo code. In order to improve the signal to noise ratio different collimators and a filter were placed between the neutron source and the object. The effect of the positioning of the neutron beam and the detector relative to the object has been studied. In this work the optimisation procedure is demonstrated for boron. Monte Carlo calculations were carried out to compare the performance of the proposed PGNAA system using four different neutron sources (^{241}Am/Be, ^{252}Cf, ^{241}Am/B, and DT neutron generator). Among the different systems the ^{252}Cf neutron based PGNAA system has the best performance.

Keywords Monte Carlo simulations · Gamma radioactivity · PGNAA

Introduction

The Prompt Gamma Ray Neutron Activation Analysis (PGNAA) technique is based upon bombarding a sample with neutrons and measurement of the prompt gamma spectrum emitted from the elements in the sample after absorbing a neutron. PGNAA technique has been widely used for analyzing bulk materials, and corresponding analyzers have been commercially available for many years. However, PGNAA suffers from relatively complicated gamma spectra and the interference from the neutron source, the structural materials and the natural background. Neutron radioactive capture reaction is a purely nuclear process and can be used for the characterization of material composition. The neutron interacts with the target nucleus and a compound nucleus is formed in excited state. The excited compound nucleus then de-excites quickly (less than 10^{-14} s) to the ground level by emitting gamma rays that are unique for each element. The most of publications using this technique are concerned for determining light elements (H, B, C, N, Si, P, S and Cl) and the elements with a large neutron capture cross sections (Cd, Sm and Gd) by irradiating them with neutrons [1–9].

For the design of a PGNAA unit, it is highly recommended to evaluate the performance of PGNAA systems utilizing a range of neutron sources such as ^{241}Am/Be, ^{252}Cf, ^{241}Am/B, and DT neutron generator [10–12]. For that reason a PGNAA facility has been simulated using the MCNPX Monte Carlo code [10]. The simulation carried out aimed to improve the signal to noise ratio. The study has a practical interest in the case of the in vivo PGNAA of boron in the human liver [13, 14] and in the determination of boron in water samples because B is one of the elements present at trace levels in water as dissolved salts [2].

Irradiation facility

The geometrical configuration of the arrangement used in the present simulation is represented in Fig. 1 and is similar to the one described previously, in Ref. 15 with a minor difference in geometry. Effectively, it comprises: (1) a cylindrical irradiation unit made of polyethylene, with a

J. G. Fantidis (✉) · C. Potolias · N. Vordos · D. V. Bandekas
Department of Electrical Engineering, Kavala Institute of Technology, Kavala, Greece
e-mail: fantidis@yahoo.gr

G. E. Nicolaou
Laboratory of Nuclear Technology, School of Engineering, 'Democritus' University of Thrace, Xanthi, Greece

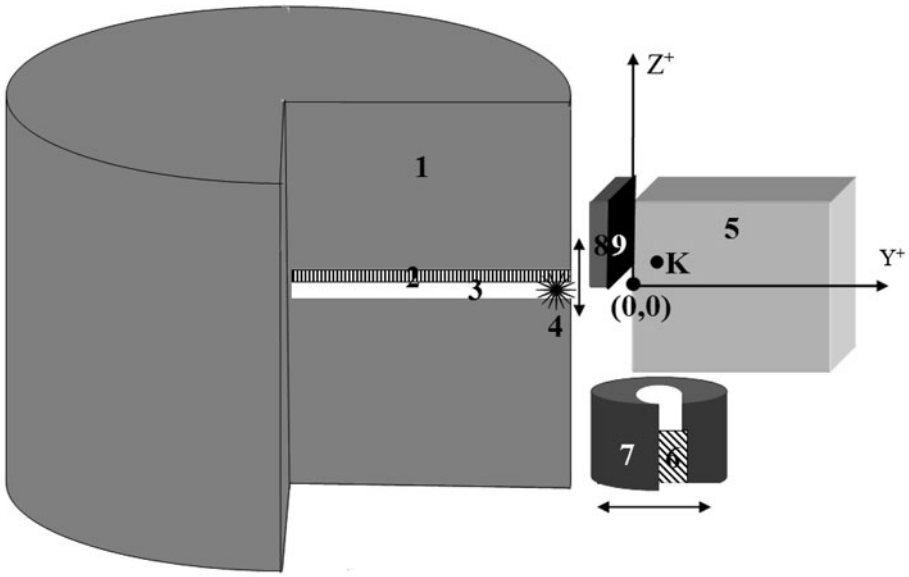

Fig. 1 3D view of the simulated experimental set-up (not in scale)

height and diameter of 100 cm, (2) a collimator made of Beryllium with 1 cm diameter, (3) a Perspex tube of length 50 cm with an inner diameter of about 1 cm runs through the *y* axis of the cylinder. The tube provides a path for the transfer of the neutron source from its resting to the irradiation position. The source can be moved between the shielded and the irradiation positions. When the unit operates (4) the source is situated near to the edge of the tube, 49 cm away from the center of the cylinder. Four different neutron sources were studied: (i) ^{241}Am/Be, (ii) ^{252}Cf, (iii) ^{241}Am/B and (iv) DT neutron generator. Normalized neutron spectra for four sources are shown in Fig. 2. The irradiation object (5) is a cubic phantom with a side of 16 cm length. The cube contains water with homogeneously distributed 40 ppm of ^{10}B. This is a typical quantity of boron in liver which is in the range of 8 to 50 ppm in the healthy and sickly liver, respectively [16, 17].

The prompt gamma rays produced in the phantom were detected using a cylindrical Ge detector (6) having a diameter and height of 5 cm. In order to prevent undesired gamma rays from reaching the detector, (7) Lead cylindrical collimator with 10 cm height and 12 cm diameter are inserted between the phantom and the detector. The gamma rays arrive to the detector through in a cylindrical aperture with 5 cm height and 4 cm diameter. The collimated detector and the neutron sources have central axes which are on the same horizontal mid-plane through the object.

In large samples the effect of self-absorption within the object is an important parameter, which depends on the photon energy, the geometry and the material of the investigated object. In the present paper the high magnitude of the peak resulting from the hydrogen prompt gamma rays is undesirable. The 2.223 MeV gamma rays from the hydrogen in the phantom are not attenuated in the object due to their larger mean free path (approximately 22 cm). In contrast the 0.478 MeV gamma rays from B has a mean free path of only 10.3 cm. It means that the above region of the phantom contributes little in the signal but increases considerably the background. In order to minimise the neutron reaction rate and thereby the magnitude of the hydrogen peak, which enhances the gamma background, a rectangular neutron filter (8) of 4.9 cm thickness and (9) a cadmium layer of 0.1 cm in thickness were placed between the neutron source and the object.

The major drawback for PGNAA is that it has a relatively low signal to noise ratio. The aim of the present work is to improve the signal to noise ratio. Collimated detectors, which are common in a variety of radiation physics situations, can 'see' only a part of the investigated object. Nicolaou et al. [18] show that in these circumstances a volume of intersection is formed by the field of view of the collimator and the neutron beam. The detector response depends on the volume of the intersection (V) and its solid angle Ω_D with the detector as well as on the reaction rate within this volume. The solid angle Ω_D can easily be calculated using a Monte Carlo method utilising total variance reduction and is given by [18–20]:

$$\Omega_D = \frac{1}{N}\sum_{i=1}^{N} W_i \tag{1}$$

where, Wi is a weighting factor related with random positions within the volume V that emit induced gamma

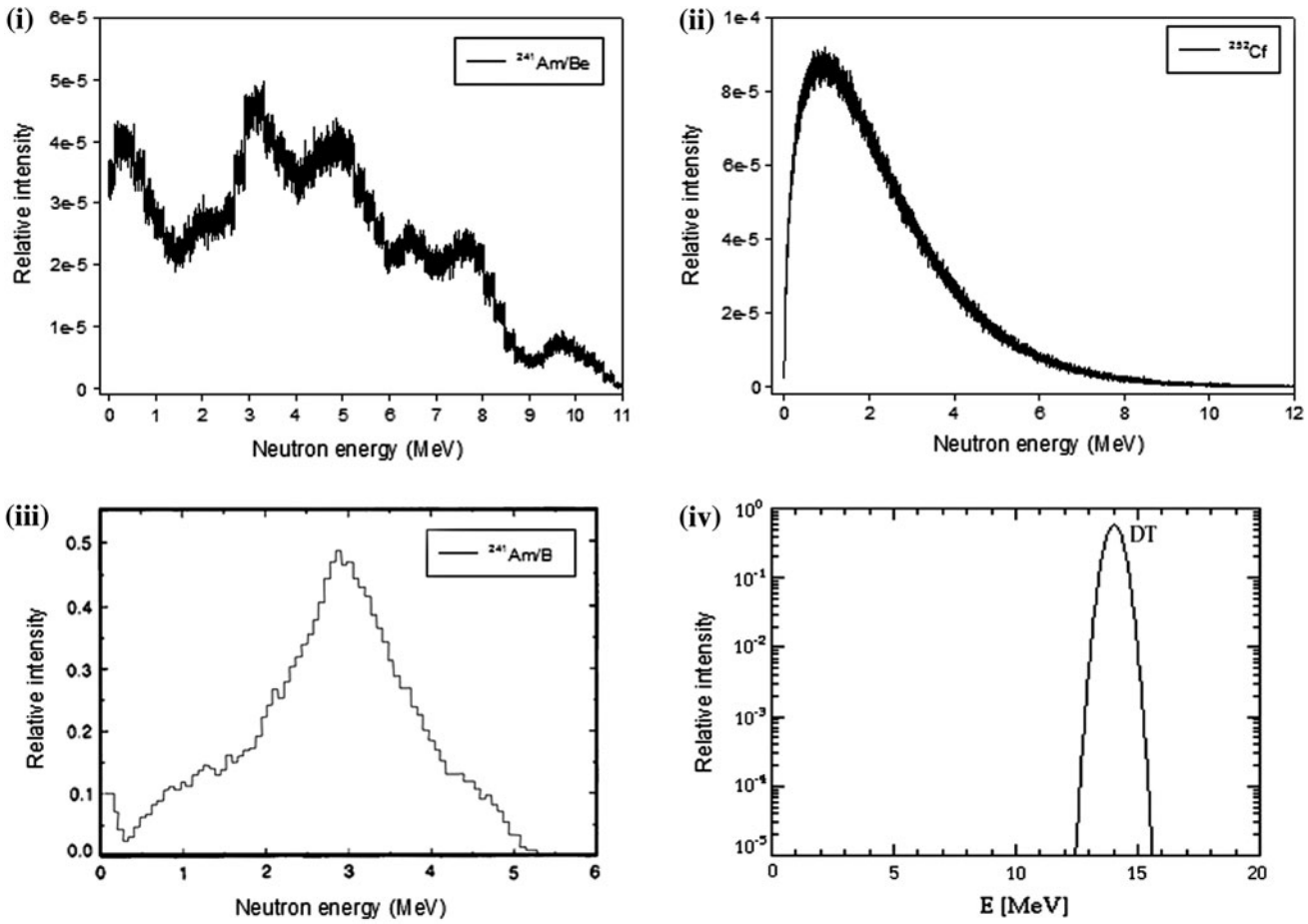

Fig. 2 Normalized neutron spectra for (i) ^{241}Am/Be, (ii) ^{252}Cf, (iii) ^{241}Am/B and (iv) DT neutron generator sources

rays and subtend a non-zero solid angle with the detector ($Wi \neq 0$) and N is the number of these positions. The improvement of the results for a ^{252}Cf neutron source has already been demonstrated by Fantidis et al. [15]. In this paper the proposed procedure and the detection sensitivity optimized for four different neutron sources are presented.

Presentation of the method

The methodology proposed in this paper comprises 3 steps: The first step is to maximize the signal, which is proportional to the thermal neutron flux in the sample, the second step is to minimize the signal background and the third is to maximize the prompt gamma ray detection efficiency. In order to reduce the reaction rate in the above region in the phantom and hence the Compton continuum due to the 2.223 MeV gamma rays, while increasing the reaction rate in the below part of the phantom, two stages were taken. Firstly, a collimator was used around the neutron path tube to reduce the divergence of the neutron beam towards the object. Secondly, a filter was placed between the neutron beam and the object in the above region of the phantom. The aim of the filter is also twofold: to moderate and absorbs neutrons towards the above region, while reflecting neutrons towards the bellow region.

A final step with a view to optimise the (boron) gamma ray detection sensitivity was carried out for different positions of the irradiation and detection parts of the unit in Fig. 1, relative to the object. The different positions of the collimated detector are along the object in the $y+$ direction, while of the neutron beam with the filter along the $z+$ and $z-$ directions.

Results and discussion

Neutron flux is one of the key factors determining the performance of PGNAA setup. With the intention to find the best collimator, which was used around the neutron path tube, the thermal neutron flux (f_{th}) was calculated with the aid of MCNPX Monte Carlo code. The f_{th} was computed using the F5:N tally, which gives the neutron flux at a point detector in neutrons cm^{-2} per starting neutron.

Calculations were performed at a point K with coordinates $z = y = 2.5$ cm for a total number of histories per starting neutron (NPS) of 5×10^6 histories yielding an accuracy of <0.5% (Table 1). An energy boundary of 0.01–0.3 eV was used to score the thermal neutron flux. The materials considered for the collimator were light water (H_2O), graphite (C), polyethylene (CH_2), beryllium (Be), and heavy water (D_2O).

The f_{th} flux at the point of interest is given in Table 1 for the different materials considered. The maximum reduction in thermal neutrons flux was achieved with Be. Therefore, a collimator, consisting of a Be layer covering the tube towards the above region of phantom (Fig. 1) was applied. Correspondingly the maximum neutron flux was achieved for CH_2 and for this reason the below part of a tube was covered by CH_2.

In order to maximize the signal to noise ratio a rectangular shaped filter was placed between the object and the neutron source (Fig. 1). The effect of the filter material on the f_{th} was calculated, using the MCNPX code, for a filter of 4.9 cm thickness consisting of different materials. The materials considered were H_2O, C, CH_2, Be, D_2O and no filter. The 0.478 MeV prompt gamma ray from the $^{10}B(n, \alpha)^7Li$ reaction, defined with the F8:P tally, was used as an optimization index in choosing the material of the filter. The F8:P is a pulse height tally giving the energy distribution of pulses created in the Ge detector, in photons/keV per starting neutron. Cutoff (NPS) values up to 5×10^7 histories were considered yielding an accuracy of <1% in the calculations.

For ^{241}Am/B and ^{241}Am/Be neutron sources the maximum number of 0.478 MeV photons in the pulse height distribution, takes place in the case of the CH_2 filter with an increase in yield by 1.05 and 1.07 correspondingly, over the cases without filter. For ^{252}Cf and DT neutron generator the maximum values occur in the case of graphite filter with an increase by factors of 1.14 and 1.12 correspondingly (Table 2).

The effect of the differenct positions between the collimated detector and the neutron sources were simulated with the MCNPX code. Again the 0.478 MeV prompt gamma ray, determined with the F8:P tally (NPS = 5×10^8 histories), was used as an optimization index for the position with the best detection sensitivity. The normalized values of the 0.478 MeV boron peak areas for the different (y, z) coordinates are given in Tables 3 and 4. Best detection sensitivity for the boron is consequently obtained positioning the detector and the neutron source at $y = 2$ cm and $z = -2$ cm, respectively for ^{241}Am/B, ^{241}Am/Be and ^{252}Cf neutron sources and at $y = 2$ cm and $z = -7$ cm for DT neutron generator ('best' positioning).

The comparison of the 'best' position with the symmetrical case with no filter of Fig. 1 was calculated on the basis of the signal to noise ratio and the associated relative error. In all circumstances an irradiation time of 1000 s with neutron flux equal to 2.3×10^6 n/s cm^2 were considered. The results from the ^{241}Am/B neutron, ^{241}Am/Be neutron, ^{252}Cf neutron and DT neutron based PGNAA system, which were calculated using the MCNPX code, are listed in Table 5. In the case of ^{241}Am/B neutron source the signal to noise ratio and the relative error have increased by factors of 1.24 and 1.22, respectively. In the case of ^{241}Am/Be neutron source the signal to noise ratio and the relative error have improved by factors of 1.32 and 1.24 correspondingly. For the ^{252}Cf neutron source the signal to noise ratio and the relative error have increased by factors of 1.33 and 1.25, respectively. For the DT neutron generator based system the signal to noise ratio and the relative error have improved by factors of 1.40 and 1.49 correspondingly.

According to the results of the simulation study (Table 5) the performance of the ^{252}Cf neutron based system is the best, even though the ^{241}Am/Be or ^{241}Am/B neutron based PGNAA system have comparable performance. However the performance of the DT neutron based system is poorer than others systems.

In order to see the effect of source positioning on neutron flux distribution, the ^{252}Cf neutron source was placed at different positions along the $z+$ and $z-$ directions (Fig. 1). Three energy ranges are considered: thermal neutrons (0.01–0.3 eV), epithermal neutrons (0.3 eV–10 keV), and fast neutrons (above 10 keV). Neutron fluxes were calculated in region #1 (Fig. 3) using the F4 tally with NPS = 10^7 histories yielding an accuracy <1%. Region #1 is a cube with a side of 8 cm, which is symmetrically placed on the x axis. It is seen that the source at $z = -2$ cm

Table 1 Thermal neutron flux ($\times 10^{-4}$ n/cm^2 per starting neutron) at point K

Source	Collimator material				
	H_2O	C	CH_2	Be	D_2O
^{241}Am/Be	4.09	4.01	4.21	2.81	4.07
^{252}Cf	5.63	5.24	5.73	3.71	5.49
^{241}Am/B	4.31	4.14	4.45	3.22	4.32
DT neutron generator	1.32	1.34	1.37	0.99	1.35

Table 2 Number of pulses at the 0.478 MeV peak ($\times 10^{-5}$ pulses/keV per starting neutron) in detector cell

Source	Filter material (4.9 cm thickness + 0.1 cm thickness Cadmium)					
	No filter	H_2O	C	CH_2	Be	D_2O
^{241}Am/Be	5.04	5.17	5.09	5.39	3.96	5.22
^{252}Cf	6.34	6.43	7.22	7.09	4.83	7.17
^{241}Am/B	5.43	5.70	5.52	5.96	4.52	5.74
DT neutron generator	1.49	1.55	1.66	1.56	1.26	1.52

Table 3 The normalized 0.478 MeV peak area, for the different positions of the ^{241}Am/B, ^{241}Am/Be and ^{252}Cf neutron sources and detector relative to the object

Detector position (Y axis)	^{241}Am/B						^{241}Am/Be						^{252}Cf					
	Neutron source position (Z axis)																	
	2	0	−1	−2	−3	−4	2	0	−1	−2	−3	−4	2	0	−1	−2	−3	−4
2	0.92	0.96	0.99	1	0.98	0.95	0.82	0.93	0.96	1	0.98	0.94	0.85	0.96	0.96	1	0.95	0.94
4	0.64	0.72	0.71	0.70	0.68	0.67	0.62	0.67	0.68	0.71	0.69	0.66	0.67	0.72	0.71	0.71	0.69	0.65
6	0.49	0.51	0.52	0.52	0.52	0.5	0.46	0.48	0.49	0.50	0.49	0.49	0.43	0.46	0.47	0.47	0.46	0.44

Table 4 The normalized 0.478 MeV peak area, for the different positions of the DT neutron generator beam and detector relative to the object

Detector position (Y axis)	DT neutron generator								
	Neutron source position (Z axis)								
	2	0	−1	−2	−3	−4	−5	−6	−7
2	0.75	0.76	0.80	0.82	0.84	0.86	0.91	0.94	1
4	0.59	0.61	0.64	0.65	0.66	0.67	0.73	0.77	0.79
6	0.46	0.48	0.5	0.51	0.52	0.53	0.54	0.59	0.63

Table 5 The comparison of the difference neutron sources for irradiation time equal to 1000 s with neutron flux equal to 2.3 × 10^6 n/s

	Source/position							
	^{241}Am/B		^{241}Am/Be		^{252}Cf		DT neutron generator	
	Symmetric	Best	Symmetric	Best	Symmetric	Best	Symmetric	Best
S	1.25E+5	1.87E+5	1.16E+5	1.79E+5	1.46E+5	2.27E+5	3.42E+4	7.84E+04
B	1.83E+3	2.64E+3	3.21E+3	4.39E+3	1.97E+3	2.69E+3	4.35E+3	1.17E+04
$S/\sqrt{B}$	2.93E+3	3.64E+3	2.05E+3	2.71E+3	3.29E+3	4.37E+3	5.18E+2	7.24E+02
r_S	2.87E−3	2.35E−3	3.01E−3	2.42E−3	2.65E−3	2.12E−3	6.06E−3	4.07E−03

is the optimum position (Fig. 4). At $z = -2$ cm the ^{252}Cf neutron source produce the highest value for the thermal and epithermal neutron flux and the lowest value for the fast fluence rate. The comparison of the neutron spectrum in region #1 between the symmetrical case with no filter and in case with source at the best positions is illustrated in Fig. 5.

The energy distribution of pulses created in the detector, as obtained using the F8 tally and GEB parameter, is shown in Fig. 6 (for the ^{252}Cf neutron source). In order to provide a spectrum similar to detector the MCNP code has a special parameter for tallies, the GEB Gaussian Energy Broadening option. The GEB can be used to better simulate a physical radiation detector in which energy peaks exhibit Gaussian energy broadening. According to the MCNPX manual the tallied energy is broadened by sampling from the Gaussian [21, 22]:

$$f(E) = Ce^{-\left(\frac{E-E_0}{A}\right)^2} \quad (2)$$

where E = the broadened energy, E_0 = the unbroadened energy of the tally, C = a normalization constant, and A = the Gaussian width. The Gaussian width is related to the full width half maximum (FWHM) by

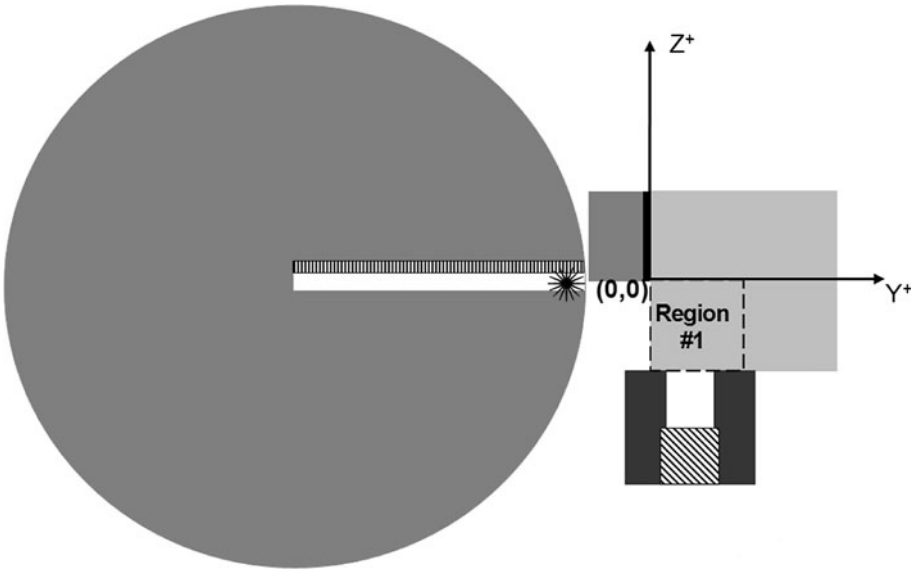

Fig. 3 Top view of the simulated experimental set-up (not in scale)

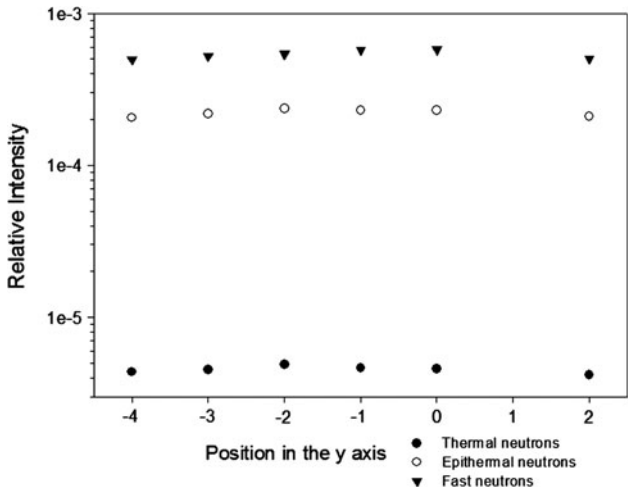

Fig. 4 The effect of source positioning on neutron flux distribution

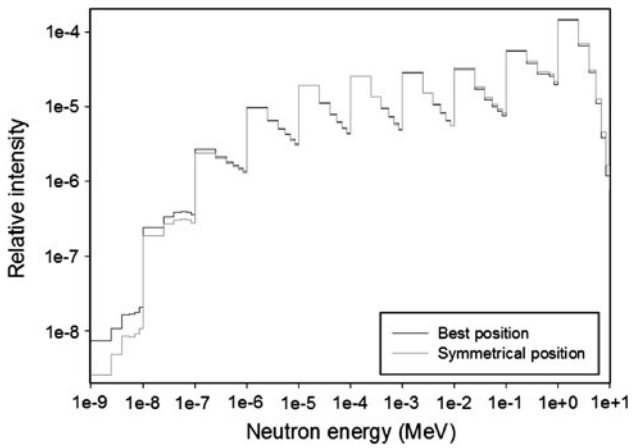

Fig. 5 The neutron spectrum in region #1 before and after the optimization procedure (for the ^{252}Cf neutron source)

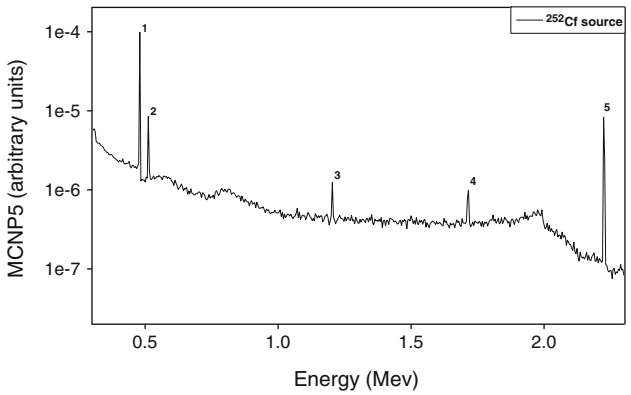

Fig. 6 Simulated energy distribution of the pulses created in the Ge detector due to the prompt gamma rays from the object

$$A = \frac{\text{FWHM}}{2\sqrt{\ln 2}} \tag{3}$$

The desired FWHM is specified by the user-provided constants, a, b, and c, where

$$\text{FWHM} = a + b\sqrt{E + cE^2} \tag{4}$$

The FWHM is defined as

$$\text{FWHM} = 2(E_{\text{FWHM}} - E_0) \tag{5}$$

where E_{FWHM} is such that $f(E_{\text{FWHM}}) = \frac{1}{2}f(E_0)$, and $f(E_0)$ is the maximum value of $f(E)$.

The full energy distribution for energies up to 2.3 MeV is shown in Fig. 6. Besides the peak due to boron (peak 2), several gamma ray peaks corresponding to neutron capture reactions with the major components in the object are identified in the spectrum: the 0.511 MeV annihilation peak (peak 1); the 2.223 MeV from the ^{1}H(n, γ)^{2}H reaction and its single and double escape peaks at 1.712 MeV and 1.201 MeV (peaks 5, 4, 3, respectively).

Table 6 The maximum total dose equivalent rate

Neutron source	^{241}Am/Be	^{252}Cf	^{241}Am/B	DT neutron generator
Dose equivalent	1.8 mSv	1.6 mSv	1.75 mSv	2.05 mSv

For every in vivo neutron activation analysis dosimetry is one of the main concerns. With respect to determine the dose, the phantom was divided into elements of 1 cm^3 volume. The total dose equivalent rate (DER), due to the neutrons and photons, was calculated with the MCNPX Monte Carlo code, using the F4, Fm4 tallies and the DE, DF cards. The F tallies describe the neutron flux within a cell, while the D cards convert the absorbed dose to equivalent dose. The total dose equivalent delivered to the phantom in the case of neutron flux of 2.3×10^6 n/s and irradiation/prompt counting times of 1000 s. In all circumstances the source was placed in the best position. The results are presented in the Table 6. The maximum total dose equivalent ranged between 1.6 and 2.05 mSv. The effective dose ranged among 80 and 102.5 μSv, with 0.05 as a value of tissue weighting factor for liver.

Conclusion

A PGNAA facility comprising an isotopic neutron source has been simulated using the Monte Carlo code MCNP. With the intention to improve the signal to noise ratio a filter placed between the neutron source and the object and different positioning of the neutron beam and the detector relative to the object analysed were considered. Performance of a ^{241}Am/Be neutron, a ^{241}Am/B neutron and a DT neutron generator neutron based PGNAA system was compared with that of a ^{252}Cf neutron based PGNAA system. The results of the simulation study showed that performance of a ^{241}Am/Be neutron based PGNAA system is comparable with that of a ^{241}Am/Be neutron based system. Both systems have performance slightly poorer than the performance of the ^{252}Cf neutron based system. However the performance of the DT neutron based PGNAA system is considerably poorer than that of the ^{252}Cf neutron based PGNAA system.

The optimization procedure demonstrated its usefulness for the in vivo of measurement of boron in the human liver. However it can be used not only for the PGNAA of other elements in liver, such as Cd (0.559 MeV) and Hg (0.368 MeV) but also in a range of elements in other bulk samples, for example soil, ore and land filled waste.

References

1. Acharya R (2009) J Radioanal Nucl Chem 281:291
2. Ramanjaneyulu PS, Sayi YS, Newton Nathaniel T, Reddy AVR, Ramakumar KL (2007) J Radioanal Nucl Chem 273:411
3. Atanackovic J, Grinyer J, Chettle DR, Byun SH (2007) Nucl Instrum Methods B 263:169
4. Blaauw M, Belgya T (2005) J Radioanal Nucl Chem 265:257
5. Ellis KJ, Shypailo RJ (2008) J Radioanal Nucl Chem 276:79
6. Stamatelatos IE, Kasviki K, Green S, Gainey M, Kalef-Ezra J, Beddoe A (2004) Anal Bioanal Chem 379:192
7. Spyrou NM (1999) J Radioanal Nucl Chem 239:59
8. Kasviki K, Stamatelatos IE, Yannakopoulou E, Papadopoulou P, Kalef-Ezra J (2007) Nucl Instrum Methods B 263:132
9. Idiri Z, Mazrou H, Amokrane A, Bedek S (2010) Nucl Instrum Methods B 268:213
10. Pelowitz DB (2005) MCNPX™ USER'S MANUAL Version 2.5.0
11. Marsh JW, Thomas DJ, Burke M (1995) Nucl Instrum Methods A 366:340
12. Reijonen J, Gicquel F, Hahto SK, King M, Lou TP, Leung KN (2005) Appl Radiat Isot 63:757
13. Sutcliffe JF (1996) Phys Med Biol 41:791
14. Chettle DR (2006) J Radioanal Nucl Chem 268:653
15. Fantidis JG, Nicolaou GE, Tsagas NF (2009) Radiat Meas 44:273
16. ICRP (2003) Basic anatomical and physiological data for use in radiological protection: reference values. ICRP-89
17. Koivunoro H, Bleuel DL, Nastasi U, Lou TP, Reijonen J, Leung KN (2004) Appl Radiat Isot 61:853
18. Nicolaou G (2006) Radiat Measur 41:213
19. Wielopolski L, Chettle DR (1977) Nucl Instrum Methods 143:577
20. Fantidis JG, Nicolaou GE, Tsagas FN (2007) Localisation and distribution of radioactivity in soil: solid angle issue. International conference on enviromental radioactivity, Vienna 22–27 April 2007, Austria
21. Venkataraman R, Croft S, Russ WR (2005) J Radioanal Nucl Chem 264:183
22. Hakimabad HM, Panjeh H, Vejdani-Noghreiyan A (2007) Appl Radiat Isot 65:918